JACS
JOURNAL OF THE AMERICAN CHEMICAL SOCIETY

Communication

pubs.acs.org/JACS

Unusual Topological RNA Architecture with an Eight-Stranded Helical Fragment Containing A-, G-, and U-Tetrads

Chao-Da Xiao,[†] Takumi Ishizuka,[†] Xiao-Qing Zhu,[†] Yue Li,[‡] Hiroshi Sugiyama,[‡] and Yan Xu*[,†]

[†]Division of Chemistry, Department of Medical Sciences, Faculty of Medicine, University of Miyazaki, 5200 Kihara, Kiyotake, Miyazaki 889-1692, Japan

[‡]Department of Chemistry, Graduate School of Science, Kyoto University, Kitashirakawa-oiwakecho, Sakyo-ku, Kyoto 606-8502, Japan

Supporting Information

ABSTRACT: Human telomeric RNA performs various cellular functions such as telomere length regulation, heterochromatin formation, and chromosome end protection. Using a combination of nuclear magnetic resonance, circular dichroism, and gel electrophoresis, we observed an unusual topological structure formed by human telomere RNA r(GUUAGGGU). Our results showed that every set of four strands formed a parallel G-quadruplex as symmetry-related units containing four G-tetrads, two U-tetrads, and one A-tetrad. An eight-stranded helical fragment containing A-, G-, and U-tetrads provided a central intercalated scaffold that connected two G-quadruplex units in an alternating antiparallel arrangement, giving rise to a novel RNA architecture. This higher order RNA structure is so stable that it would be surprising if similar structures do not occur in nature. Our findings provide a new insight into the behavior of human telomeric RNA molecules.

Telomeric RNA molecules have been found in various human and rodent cell lines.[1] The existence of telomeric RNA has added a new level of complexity in the regulatory and protective mechanisms of chromosome ends. Telomeric RNA has been shown to be involved in various cellular functions, such as regulating telomere length and forming telomeric heterochromatin.[2] Recently, we demonstrated that telomeric RNA G-quadruplex plays an important role in providing a protective structure for telomere ends.[3] Defining the structural features of telomere RNA will be essential to understanding telomere biology and telomere-related diseases.

To achieve this goal, we investigated the structure and molecular size of human telomere RNA sequence r(G1U2U3A4G5G6G7U8) (ORN-1, 8-nt) by gel electrophoresis under nondenaturing and denaturing conditions. Under nondenaturing conditions, ORN-1 migrated slower than the reference DNA dT24 and the reported 12-nt telomere RNA G-quadruplex (Figure 1a),[4] indicating that ORN-1 adopted a higher order structure. Surprisingly, ORN-1 showed similar mobility in denaturing gel electrophoresis, indicating that its structure remained stable against base-pair hydrogen-bond disruption by urea in denaturing condition (Figure 1b). These data indicate that ORN-1 formed a very stable, higher order RNA architecture in Na^+ solution.

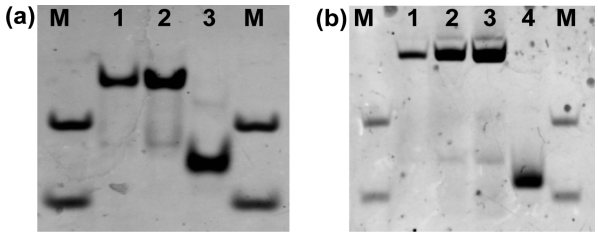

Figure 1. (a) Nondenaturing gel electrophoresis of ORN-1. Lane M, makers dT12 and dT24; lane 1 and 2, ORN-1 (100 and 200 pmol); lane 3, 12-nt $r(UAGGGU)_2$. (b) Denaturing gel electrophoresis of ORN-1. Lane M, makers dT12 and dT24; lane 1, 2, and 3, ORN-1 (50, 100, and 200 pmol); lane 4, 12-nt $r(UAGGGU)_2$.

Initial investigation of ORN-1 by circular dichroism (CD) spectroscopy revealed a positive band at 265 nm and a negative band at 240 nm (Supporting Information, Figure S1a), which are characteristics of CD spectra for parallel G-quadruplex structures.[5] We next examined the thermal stability of ORN-1 by CD spectroscopy temperature melt (Figure S1b). The resulting melting profile showed that the folded RNA architecture of ORN-1 had high thermal stability, with a melting temperature (T_m) higher than 90 °C in Na^+ solution. Such high T_m is remarkable for RNA G-quadruplexes stabilized by Na^+ ions, and is generally only observed for RNA G-quadruplexes stabilized by K^+ ions.[6]

To reveal the detailed structure of ORN-1, we performed nuclear magnetic resonance (NMR) experiments. We observed six imino peaks in the imino proton region of the ^1H NMR spectrum of ORN-1 in the presence of Na^+, indicating the G-quadruplex structure formed by ORN-1 to be far more complex than initially assumed, in which a twice higher intensity peak presented by two overlapped peaks (marked by asterisk) (Figure 2). Because all strands of ORN-1 in a parallel G-quadruplex were equivalent, three G-tetrad rings by G5, G6, and G7 should have resulted in three imino proton signals. Therefore, the presence of six imino peaks indicates that there were more than three G-tetrads in the structure; additional tetrads possibly included a fourth G-tetrad formed by G1, or A- and U-tetrads formed by A4 and U2, 3, 8, respectively. The imino peaks are observed even at 80 °C at a temperature-

Received: December 4, 2016
Published: February 8, 2017

DOI: 10.1021/jacs.6b12274
J. Am. Chem. Soc. 2017, 139, 2565−2568

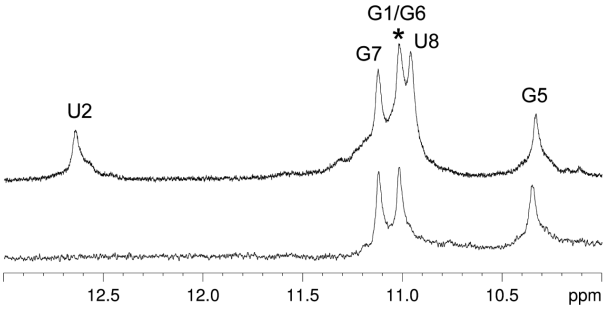

Figure 2. Imino proton NMR spectra of ORN-1 in the presence of 100 mM NaCl and 10 mM Na-phosphate buffer (pH 6.8), 25 °C. Asterisk indicates the overlapped two peaks. Top spectrum was recorded in H_2O; bottom spectrum was recorded after 1 month in D_2O.

dependent experiment (Figure S2), confirming a highly stable structure that is consistent with the results of gel electrophoresis and CD.

To examine the above hypothesis and to understand further the structure of ORN-1 G-quadruplex, we performed NMR spectral assignment by a combination of hydrogen−deuterium exchange (HDX),[7] homonuclear NOESY, and heteronuclear [^{13}C−^{1}H] HMBC experiments at natural abundance.[4b,8]

In consistency with the results of gel electrophoresis and temperature melt, further indication of the stability of ORN-1 G-quadruplex comes from the observation that its imino protons remained detectable in the HDX experiment even after 1 month of incubation in D_2O (Figure 2). Sequential assignments of G1 to U8 of ORN-1 were derived from tracing the H8/H6−H1′ sequential connectivity in the NOESY spectrum (Figure 3a). We also analyzed the spectra of sequences containing single, site-specific substitutions where rG, rA, and rU were replaced by dG, dA, and dT, respectively (Table S1, Figure S3).[4b] These substitutions allowed us to unambiguously validate our proton assignments. As an example of the spectroscopic effects of these substitutions, the DT3 (dT-for-rU substitution), H2′, and H2″ protons of the substituted residue were shifted upfield and were thus easily recognizable (at ∼2 ppm) (Figure S4) whereas the unchanged NOE patterns and imino peaks indicate that the single substitution did not perturb the overall higher order structure (Figures S1, 3 and 4). The imino protons assignments were based on the through-bond correlation between H8 and imino protons via ^{13}C5 at natural abundance of each individual rG (Figure S5).[4b,8] The intratetrad NOE connections G1H1−G1H8, G5H1−G5H8, G6H1−G6H8, and G7H1−G7H8 revealed the formation of four G-tetrads (Figure 3b,f).

The imino proton of U2 that gave NOEs to H5 and H6 resonances provides evidence for the formation of U-tetrad (Figure 3c,g). The fixed intramolecular distance of imino proton (H3) to H6 (>5 Å) is unable to give an NOE cross peak, which in turn indicates that the NOE cross peak from the imino proton (H3) to H6 must have been an intermolecular signal of U in the U−U base pair. Furthermore, the strong

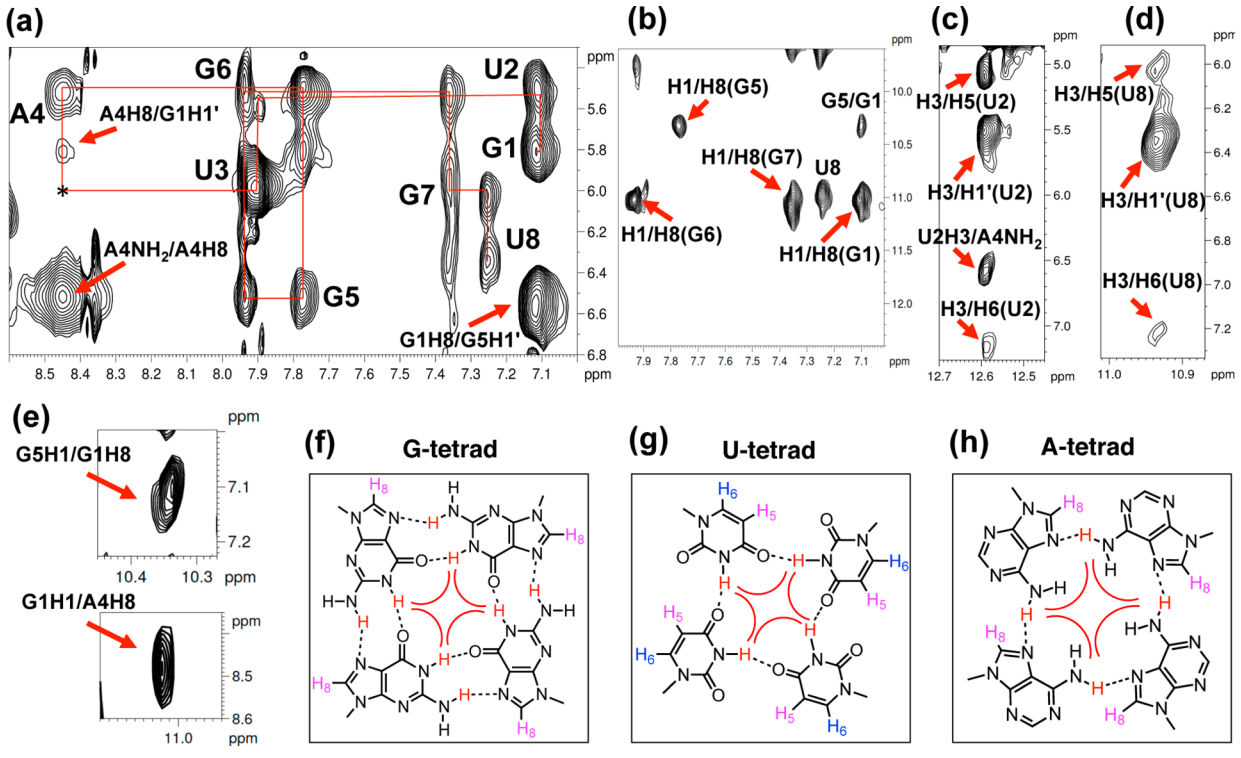

Figure 3. (a) H8/H6−H1′ proton region of NOESY spectrum (mixing time, 300 ms) of ORN-1 in Na^+ solution. The sequential pathway is shown (red line). Intraresidue H6/H8−H1′ NOE cross-peaks are labeled with residue numbers. Cross peaks A4NH$_2$−A4H8, G1H8−G5H1′, and A4H8−G1H1′ are shown. (b) Imino−H8 (G) proton region of NOESY spectrum of ORN-1. (c) H3−H5/H6 (U2) proton region of NOESY spectrum of ORN-1. Cross peaks for H3−H5 (U2), H3−H1′ (U2), and H3−H6 (U2) are shown. Cross peak for U2H3−A4NH$_2$ is indicated. (d) H3−H5/H6 (U8) proton region of NOESY spectrum of ORN-1. Cross peaks for H3−H6 (U8), H3−H1′ (U8), and H3−H5 (U8) are shown. (e) NOE peaks G5H1−G1H8 and G1H1−A4H8 for stacking between two G-quadruplex units. (f) Illustration structure of G-tetrad. (g) U-tetrad is formed by hydrogen bonds between adjacent uridines. The hydrogens of H3, H5, and H6 are represented by red, pink, and blue colors. (h) Illustration structure of A-tetrad. The hydrogens of NH$_2$ and H8 are colored in red and pink.

DOI: 10.1021/jacs.6b12274
J. Am. Chem. Soc. 2017, 139, 2565−2568

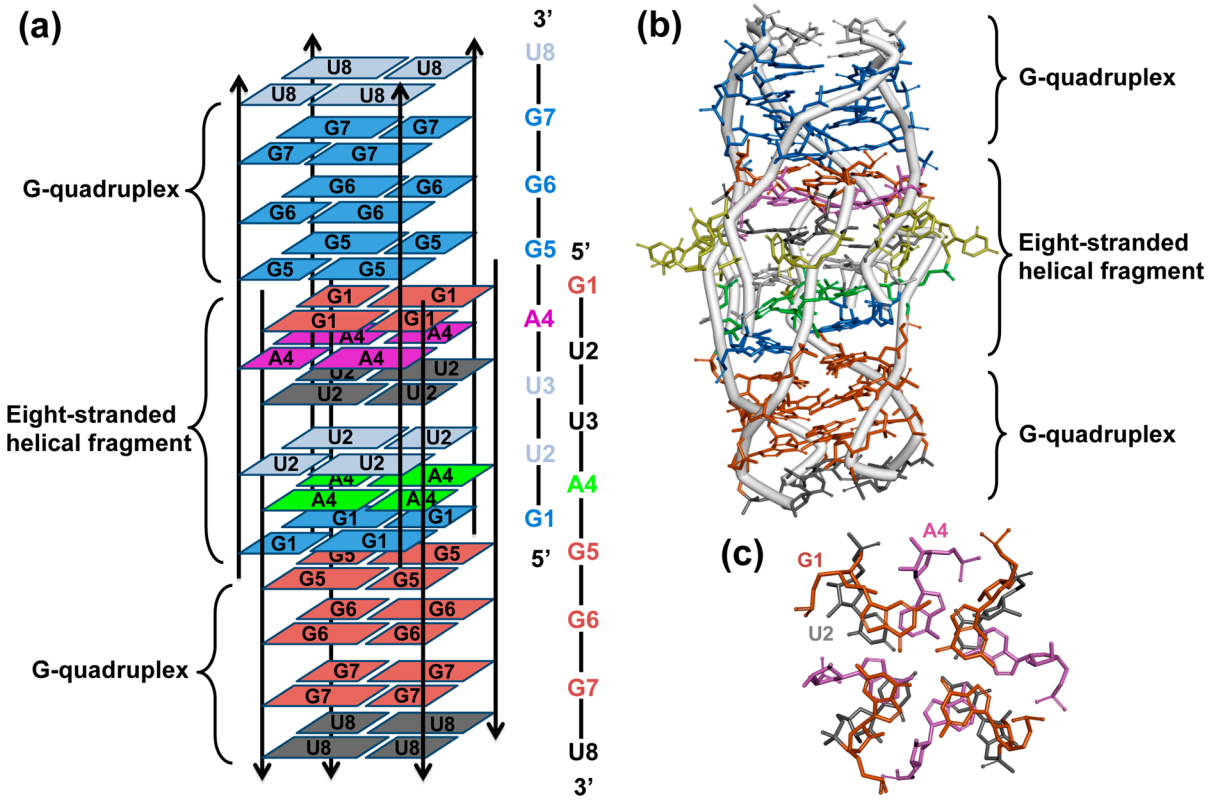

Figure 4. (a) Schematic structure of ORN-1. For clarity, G-tetrads from two G-quadruplex units are colored in red and blue; A-tetrads are colored in purple and green; U-tetrads are in black and soft blue. The residue numbers in neighbor strands are illustrated in different colors for clarity. G-quadruplex and eight-stranded helical fragment are indicated. U3 that does not form tetrad is omitted. (b) Ribbon view of the higher order structure. Tetrads were colored in the same way as panel a. U-bulges are in yellow. (c) Base-tetrad stacking in the intercalated region. Stacking of G1-, A4-, and U2-tetrads is colored in the same way as in panel a.

NOE from the imino proton to H5 must have been an intermolecular signal of U moieties, because the fixed intramolecular distance of imino proton to H5 in U (≈ 4.22 Å) could not have produced such a strong NOE.[6b] A similar result was observed on U8, as shown in Figure 3d. Therefore, the observed NOEs indicate the presence of hydrogen bonds in U−U base pairs and provide unequivocal evidence for U-tetrads formed by U2 and U8 in the higher order structure (Figure 3g, Figure S6). On the other hand, we did not observe the imino proton signal of U3 and the NOE signal between U3 and A4 in the H8/H6−H1′ region, which suggested that the U3 did not form the U tetrad. In the NOESY spectrum of ORN-1 (Figure 3a), we observed an intense cross peak from A4NH$_2$ to A4H8. For an A-base, the intramolecular distances from NH$_2$ to H8 is >4.5 Å; hence, one would not expect to observe these NOE cross peaks. Therefore, it appears that the observed cross peak was derived from the interstrand interaction of A-bases arranged in a tetrad (Figure 3h).[9]

In addition to the U- and A-tetrad, we found an intercalated fragment that is key to connect the novel RNA architecture. An eight-stranded helical fragment, which consisted of alternating antiparallel arrangement of two G-quadruplex subunits, was composed of two G-tetrads, two U-tetrads, and two A-tetrads. The NOEs were observed for G1H8−G5H1′ (Figure 3a) and G5H1−G1H8 (Figure 3e), as well as for G1H1−A4H8 (Figure 3e) and A4H8−G1H1′ (Figure 3a). These cross peaks indicate that the G-tetrad formed by G1 at one G-quadruplex was inserted between the G-tetrad (formed by G5) and the A-tetrad (formed by A4) of another G-quadruplex. Moreover, the NOE cross peak between U2H3 and A4NH$_2$ (Figure 3c) could have only occurred across the stacking interaction between the U-tetrad (formed by U2) and the A-tetrad of two G-quadruplexes. Thus, the fragment in the central region of the novel structure can be viewed as an asymmetrical doubling of a triple-tetrad block of A-, G-, and U-tetrads (Figure 4). To confirm further the intercalated fragment, we mutated the ORN-1 in each one base of G1, A4, and U2 in intercalation region using thymidine substitution and showed that the mutant sequences cannot form the unique structure (Figure S7−9).

In addition, we can still observe the higher order structure at the low concentrations, which suggested that the structure forms at the physiologically relevant concentrations (Figures S10−12).

In the proposed model, the novel RNA structural motif consists of 14 stacks of G-quartets, U-quartets, and A-quartets (Figure 4b, Figures S13−14). The G1-, A4-, and U2-tetrads are involved in formation of the eight-stranded helical fragment (Figure 4c), and U3 is bulged out in the intercalation region (Figure 4b, Figure S15).

The discovery of telomere RNA molecules opens doors to understand better the essential biological role of telomeres. At the same time, there is also a clear need to revisit structural and functional mechanisms of telomeres. We and two other groups have directed our efforts toward the identification of folding topologies for telomere RNA structures.[10] In this study, we found a unique RNA architecture formed by human telomeric RNA r(GUUAGGGU). An eight-stranded helical fragment containing A-, G- and U-tetrads provided a central intercalated

DOI: 10.1021/jacs.6b12274
J. Am. Chem. Soc. 2017, 139, 2565−2568

scaffold for stabilizing the higher order structure, in which two G-quadruplex units assembled in alternating antiparallel orientation. Each set of four strands formed a parallel G-quadruplex with symmetry-related units involving A-, G-, and U-tetrads. These observations increase the knowledge of base intercalation that is reported at a four-stranded I-motif formed with fully intercalated parallel-stranded duplexes using a $C-C^+$ base pair (C-tetrad-like).[11] This novel RNA architecture is very stable with a melting temperature over 90 °C, even under denaturing condition. Its unique structural feature adds considerably to our understanding the diversity of RNA architectures.[12] This information is important for research on the biological functions of telomere RNA and for the design of new drugs that target telomere RNA.

■ ASSOCIATED CONTENT

Supporting Information

The Supporting Information is available free of charge on the ACS Publications website at DOI: 10.1021/jacs.6b12274.

Detailed experimental procedures, gel, CD, and NMR data (PDF)

■ AUTHOR INFORMATION

Corresponding Author

*xuyan@med.miyazaki-u.ac.jp

ORCID

Yan Xu: 0000-0003-0379-8866

Notes

The authors declare no competing financial interest.

■ ACKNOWLEDGMENTS

C.-D.X. is supported by The Uehara Memorial Foundation Fellowship. T.I. is supported by JSPS KAKENHI (16K17938). This work is funded by JSPS KAKENHI (26288083) to Y.X. Support from the Takeda Science Foundation is also acknowledged.

■ REFERENCES

(1) (a) Azzalin, C. M.; Reichenbach, P.; Khoriauli, L.; Lingner, J.; Giulotto, E. *Science* **2007**, *318*, 798−801. (b) Schoeftner, S.; Blasco, M. A. *Nat. Cell Biol.* **2008**, *10*, 228−236.

(2) Schoeftner, S.; Blasco, M. A. *EMBO J.* **2009**, *28*, 2323−2336.

(3) Xu, Y.; Ishizuka, T.; Yang, J.; Ito, K.; Katada, H.; Komiyama, M.; Hayashi, T. *J. Biol. Chem.* **2012**, *287*, 41787−41796.

(4) (a) Xu, Y.; Kaminaga, K.; Komiyama, M. *J. Am. Chem. Soc.* **2008**, *130*, 11179−11184. (b) Martadinata, H.; Phan, A. T. *J. Am. Chem. Soc.* **2009**, *131*, 2570−2578.

(5) (a) Sutherland, C.; Cui, Y.; Mao, H.; Hurley, L. H. *J. Am. Chem. Soc.* **2016**, *138*, 14138−14151. (b) Dash, J.; Shirude, P. S.; Hsu, S. T.; Balasubramanian, S. *J. Am. Chem. Soc.* **2008**, *130*, 15950−15956. (c) Palumbo, S. L.; Ebbinghaus, S. W.; Hurley, L. H. *J. Am. Chem. Soc.* **2009**, *131*, 10878−10891. (d) Ambrus, A.; Chen, D.; Dai, J.; Bialis, T.; Jones, R. A.; Yang, D. *Nucleic Acids Res.* **2006**, *34*, 2723−2735.

(6) (a) Agarwala, P.; Pandey, S.; Maiti, S. *Org. Biomol. Chem.* **2015**, *13*, 5570−5585. (b) Xu, Y.; Ishizuka, T.; Kimura, T.; Komiyama, M. *J. Am. Chem. Soc.* **2010**, *132*, 7231−7233. (c) Zhang, A. Y.; Bugaut, A.; Balasubramanian, S. *Biochemistry* **2011**, *50*, 7251−7258.

(7) Hsu, S. T.; Varnai, P.; Bugaut, A.; Reszka, A. P.; Neidle, S.; Balasubramanian, S. *J. Am. Chem. Soc.* **2009**, *131*, 13399−13409.

(8) (a) Phan, A. T. *J. Biomol. NMR* **2000**, *16*, 175−178. (b) Phan, A. T.; Gueron, M.; Leroy, J. L. *Methods Enzymol.* **2001**, *338*, 341−371.

(9) Patel, P. K.; Koti, A. S.; Hosur, R. V. *Nucleic Acids Res.* **1999**, *27*, 3836−3843.

(10) (a) Xu, Y.; Suzuki, Y.; Ito, K.; Komiyama, M. *Proc. Natl. Acad. Sci. U. S. A.* **2010**, *107*, 14579−14584. (b) Collie, G. W.; Haider, S. M.; Neidle, S.; Parkinson, G. N. *Nucleic Acids Res.* **2010**, *38*, 5569−5580. (c) Xu, Y. *Chem. Soc. Rev.* **2011**, *40*, 2719−2740.

(11) Gehring, K.; Leroy, J. L.; Gueron, M. *Nature* **1993**, *363*, 561−565.

(12) Deng, J.; Xiong, Y.; Sundaralingam, M. *Proc. Natl. Acad. Sci. U. S. A.* **2001**, *98*, 13665−13670.

DOI: 10.1021/jacs.6b12274
J. Am. Chem. Soc. 2017, 139, 2565−2568